The reduced susceptibility of mouse keratinocytes to retinoic acid may be involved in the keratinization of oral and esophageal mucosal epithelium

Shoji Miyazono[1], Takahito Otani[2], Kayoko Ogata[2], Norio Kitagawa[2], Hiroshi Iida[3], Yuko Inai[4], Takashi Matsuura [1], Tetsuichiro Inai*, [2]

[1]Department of Oral Rehabilitation, Fukuoka Dental College, 2-15-1 Tamura, Sawara-ku, Fukuoka 814-0193, Japan

[2]Department of Morphological Biology, Fukuoka Dental College, 2-15-1 Tamura, Sawara-ku, Fukuoka 814-0193, Japan

[3]Laboratory of Zoology, Graduate School of Agriculture, Kyushu University, 744 Motooka, Nishi-ku, Fukuoka 819-0395, Japan

[4]Division of General Dentistry, Kyushu University Hospital, 3-1-1 Maidashi, Higashi-ku, Fukuoka 812-8582, Japan

*Corresponding author: Tetsuichiro Inai, D.D.S., Ph.D., Department of Morphological Biology, Fukuoka Dental College, 2-15-1 Tamura, Sawara-ku, Fukuoka 814-0193, Japan

Tel: +81-92-801-0411 Ext. 683, Fax: +81-92-801-4909

E-mail address: tinaitj@college.fdcnet.ac.jp, ORCID: 0000-0002-3684-960X

Abstract

Keratinocytes take up serum-derived retinol (vitamin A) and metabolize it to all-*trans*-retinoic

acid (atRA), which binds to the nuclear retinoic acid receptor (RAR). We previously reported

that serum affected keratinocyte differentiation and function; namely, it inhibited

keratinization, decreased loricrin (LOR) and claudin (CLDN) 1 expression, increased keratin

(K) 4 and CLDN4 levels, and reduced paracellular permeability in three-dimensional (3D)

cultures of mouse keratinocytes (COCA). Contrarily, RAR inhibition reversed these changes.

Here, we aimed to examine whether atRA exerted the same effects as serum, and whether it

was involved in the differential oral mucosa keratinization among animal species. Porcine oral

mucosal keratinocytes, which form non-keratinized epithelium in vivo, established

keratinized epithelium in 3D cultures. Both mouse and porcine sera induced non-keratinized

epithelium at 0.1% in COCA 3D cultures. Although atRA caused the same changes as serum,

its effective concentration differed. atRA inhibited keratinization at 0.1 nM and 1 nM in

porcine or human keratinocytes and COCA, respectively. Furthermore, atRA upregulated

CLDN7 in the cytoplasm but not in cell-cell contacts. These atRA-induced changes were

reverted by RAR inhibition. The results indicate that serum-induced changes are probably due

to the effect of serum-derived atRA, and that mouse keratinocytes require higher atRA

concentrations to suppress keratinization than porcine and human keratinocytes. We propose

that the lower susceptibility of mouse keratinocytes to atRA, rather than a lower retinol

concentration, is a possible reason for the keratinization of mouse oral mucosal epithelium.

Introduction

The oral cavity (except for the gingiva, hard palate, and filiform papillae of the tongue) and esophagus are covered by non-keratinized stratified squamous epithelium in humans, pigs, and cattle and by keratinized stratified squamous epithelium in rodents including mice and rats. However, little is known about the mechanism underlying the differences in oral and esophageal mucosal epithelium keratinization among animal species.

Keratins (K) form intermediate filaments in epithelial cells. K4, expressed in suprabasal cells, is a marker for non-keratinized stratified epithelium (Moll et al. 2008). Meanwhile, loricrin (LOR) is a marker for keratinized stratified epithelium (Hohl et al. 1993) and forms the cornified envelope in combination with other proteins.

Tight junctions are multiprotein complexes consisting of transmembrane and cytosolic plaque proteins including claudin (CLDN), occludin, tricellulin, zonula occludens (ZO)-1, ZO-2, and ZO-3. Tight junctions form a paracellular permeability barrier regulating the passage of solutes and water through the paracellular pathway. CLDNs, which include

3

more than 20 members, are essential structural and functional components of tight junctions, because exogeneous expression of CLDN1 or CLDN2 in fibroblasts was sufficient to reconstitute tight junction strands observed by freeze-fracture electron microscopy (Furuse et al. 1998). CLDN1 reconstituted smooth strands formed by the fusion of intramembranous particles on the protoplasmic face (P-face) and grooves without particles on the exoplasmic face (E-face), whereas CLDN2 formed chains of particles on grooves at the E-face and discrete scattered particles on the P-face. When CLDN1 and CLDN2 were co-expressed in fibroblasts, they copolymerized into tight junction strands and induced an intermediate type of tight junction strands/grooves with discrete scattered particles observed on both faces (Furuse et al. 1999). Notably, CLDN1 acts as a sealing CLDN that increases transepithelial electrical resistance (TER) (Inai et al. 1999), whereas CLDN2 acts as a pore-forming CLDN that creates cation-permeable, paracellular pores (Yu et al. 2009). The expression profiles of CLDN differ among tissues and determine the tissue-specific paracellular permeability barrier.

CLDN 1, 4, and 7 are differentially localized from the basal to the granular layer of the epidermis (Kirschner and Brandner 2012) and from the basal to the superficial layer of non-keratinized stratified epithelium (Babkair et al. 2016; Ban et al. 2003b; Nakatsukasa et al. 2010; Oshima et al. 2011; Oshima et al. 2012; Takaoka et al. 2007; Yoshida et al. 2009). Although the tight junction-forming proteins CLDNs are localized widely in the stratified epithelium,

tight junctions are formed in the granular cell layers of the epidermis (Furuse et al. 2002; Kubo

et al. 2009; Tsuruta et al. 2002) and superficial layers of non-keratinized stratified epithelium.

Thus, tight junctions are not always formed through the localization of one or more members

of the CLDN family in the plasma membrane. In contrast to CLDNs, occludin is a good marker

for tight junctions, because it is incorporated into tight junction strands formed by CLDN

(Furuse et al. 1998). In fact, occludin is restricted to the granular cell layer of the epidermis

(Morita et al. 1998), superficial layer of the cornea (Ban et al. 2003b), and 3D cultures of corneal

epithelial cells (Ban et al. 2003a).

Retinol, an essential nutrient, plays a role in the growth, differentiation, reproduction,

vision, and maintenance of epithelium. Retinol is taken up by cells and metabolized to

retinoic acid via retinaldehyde (Chlapek et al. 2018). All-*trans*-retinoic acid (atRA), one of the

isomers of RA including 9-cis-RA and 13-cis-RA, is the major physiologically active retinol

metabolite. atRA acts by binding to the retinoic acid receptor (RAR) in the nucleus (Giguere

et al. 1987).

Recently, we reported that 0.1% fetal bovine serum concomitantly suppressed

keratinization and LOR expression and increased K4 levels in COCA 3D cultures; moreover,

these changes were reverted by BMS 493-induced RAR inhibition (Ozaki et al. 2019). In the

presence of serum, CLDN1 disappeared from tight junctions, where occludin was localized,

whereas CLDN4 appeared around the cell boundaries of suprabasal cell layers in addition to

5

tight junctions. We speculated that these changes were probably induced by retinol in serum.

We also hypothesized that mouse serum might suppress keratinization less effectively than

porcine serum or that mouse keratinocytes might be less susceptible to atRA than porcine

keratinocytes.

The present study investigated whether: (1) mouse serum and porcine serum have

different effects on the keratinization of COCA 3D cultures, (2) porcine alveolar mucosal

keratinocytes, which form non-keratinized stratified squamous epithelium in vivo, have the

ability to establish keratinized stratified squamous epithelium in 3D cultures, (3) keratinocytes

in pig, human, and mouse differ in their keratinization-suppressing atRA concentration in 3D

cultures, (4) atRA has the same effect as serum on the protein expression and localization of

K4, LOR, CLDN 1, 4, and 7, and the barrier function in COCA 3D cultures, and (5) BMS

493-induced RAR inhibition can restore atRA-induced changes to the same level as in the

control culture.

Materials and methods

Antibodies

The following primary antibodies were used in this study: mouse anti-occludin (clone OC-

3F10, #33-1500) and rabbit anti-CLDN1 (#51-9000) antibodies from Zymed (San Francisco,

CA, USA); rabbit anti-CLDN4 (ab53156) antibody from Abcam (Cambridge, UK); rabbit

anti-CLDN7 antibody from IBL (Takasaki, Japan); mouse anti-K4 (clone 5H5, #WH0003851M1) and rabbit anti-actin (#A2066) antibodies from Sigma-Aldrich (St. Louis, MO, USA); and rabbit anti-LOR (clone 19051, #905104) antibody from BioLegend (San Diego, CA, USA). The specificity of these antibodies had been examined previously (Nikaido et al. 2019; Ozaki et al. 2019).

Cell culture media

EpiLife medium (Gibco, Grand Island, NY, USA) was supplemented with human keratinocyte growth supplement (Gibco) consisting of 0.2% bovine pituitary extract, 5 μg/ml bovine insulin, 0.18 μg/ml hydrocortisone, 5 μg/ml bovine transferrin, and 0.2 ng/ml human EGF. CnT-PR (CELLnTEC, Bern, Switzerland) and EpiLife are low calcium growth mediums, containing 70 μM and 60 μM $CaCl_2$, respectively. For 3D cultures (Seo et al. 2016), cells were cultured in each growth medium supplemented with 1.2 mM $CaCl_2$ (Nacalai Tesque, Kyoto, Japan), 10 ng/ml human keratinocyte growth factor (KGF; PeproTech, Rocky Hill, NJ, USA), and 0.283 mM L-ascorbic acid phosphate magnesium salt *n*-hydrate (Wako, Osaka, Japan), a stable derivative of ascorbic acid.

Isolation of primary porcine keratinocytes from mandibular alveolar mucosa

Pig mandibles were obtained from a slaughter house. The lingual alveolar mucosa fragment

(~3.5 cm × ~0.4 cm) was removed after serial disinfection with 10% povidone iodine and

70% ethanol, washed with CnT-PR in a 15 ml tube, and incubated overnight at 4°C in CnT-

PR containing 5 mg/ml dispase (Godoshusei, Tokyo, Japan), 200 units/ml penicillin, 0.2

mg/ml streptomycin, and 0.5 μg/ml amphotericin B prepared from 100× antibiotic /

antimycotic solution (Sigma-Aldrich) in a horizontal orientation with gentle rocking. While

maintaining the mucosa submerged in CnT-PR in a petri dish, the mucous epithelium was

gently separated from the mucosal lamina propria with two pairs of forceps. The mucosal

epithelium was incubated for 20–30 min at room temperature in 10 ml of 0.25% trypsin and 1

mM EDTA solution (Gibco) in a 50 ml tube with agitation. After incubation, the cell

suspension was filtrated through a fine tea strainer and centrifuged. The collected cells (~2 ×

10^6 cells) in 10 ml CnT-PR were plated in a collagen-coated 10-cm dish, which was prepared

by using 0.3 mg/ml native collagen acidic solution (Cellgen I-AC; Koken, Tokyo, Japan).

Cells were passaged at a ratio of 1:2 to 1:3 after reaching 70% to 90% confluency. The culture

medium was changed every 2 days.

COCA and HEKa cell culture

A murine epidermal keratinocyte cell line, COCA (Segrelles et al. 2011), was derived from

the back skin of adult C57BL/DBA mice and cultured in CnT-PR. The COCA cell line was

purchased from ECACC (Salisbury, UK). Primary human epidermal keratinocytes isolated

from adult skin, HEKa (Gibco), were cultured in EpiLife medium. Cells were passaged at a

ratio of 1:2 to 1:3, when they reached 70% to 90% confluency. Culture medium was changed

every 2 days.

3D cultures of HEKa, COCA, and primary pig keratinocytes

Cell suspensions of HEKa, COCA, or pig keratinocytes ($1.0–2.0 \times 10^6$ cells/ml) in growth

medium were seeded in cell culture inserts (0.4 μm polycarbonate filter, 12 mm diameter),

which were purchased from Merck Millipore (Darmstadt, Germany), in 24-well plates. Each

insert and well contained 0.4 ml cell suspension ($4.0–8.0 \times 10^5$ cells) and 0.6 ml growth

medium, respectively. Cells were cultured for 1–2 days, until they reached 100% confluence.

The growth medium inside and outside of the insert was replaced with 3D medium (EpiLife-

3D or CnT-PR-3D), and the cells were cultured for 16–24 h to form intercellular adhesion

structures. Then, the inserts were transferred to a 12-well plate (up to one insert), 6-well plate

(up to three inserts), or 60-mm culture dish (up to six inserts) containing 0.6 ml, 1.5 ml, or 3.2

ml 3D medium, respectively; next, airlifted cultures were established by removing the 3D

medium in the inserts. The surfaces within the inserts were kept dry following the airlift by

removing excess 3D medium. The medium was changed every 2 days, and the air–liquid

interface cultures were maintained for up to 2 weeks. In some cases, mouse serum (Nippon

Bio-Test Laboratories Inc., Saitama, Japan), porcine serum (Nippon Bio-Test Laboratories

Inc.), atRA (Sigma-Aldrich), or BMS 493 (Cayman, Ann Arbor, MI, USA), an inhibitor of

pan-retinoic acid receptors (pan-RARs), was added to the 3D medium. Stock solutions for

atRA and BMS 493 in dimethyl sulfoxide (DMSO) were prepared at concentrations of 1 μM

or 1 mM, respectively.

Immunofluorescence microscopy

After washing in phosphate-buffered saline (PBS), the 3D cultures were fixed with 1%

paraformaldehyde in PBS for 1 h at 4°C and washed with PBS. Filters with cultured cells

were cut off from the inserts. Porcine oral mucosa, containing the boundary of the lower

lingual gingiva and alveolar mucosa, was obtained from slaughter facilities, fixed with 1%

paraformaldehyde in PBS for 1 h at 4°C, and washed with PBS. Then, the mucosa was

sequentially soaked in 10%, 20%, and 30% sucrose in PBS at 4°C for 1–3 h each and

embedded in an OCT compound (Sakura Finetek Japan, Tokyo, Japan). Cryosections (5 μm)

were cut and mounted on glass slides. Some sections were stained with hematoxylin and eosin

(HE). Cryosections were washed with PBS and incubated with 0.2% Triton-X 100 in PBS for

15 min for permeabilization. Subsequently, the sections were washed with PBS and incubated

with 1% bovine serum albumin in PBS (BSA-PBS) for 15 min to block nonspecific binding.

They were then incubated with primary antibodies diluted in BSA-PBS for 1 h in a moist

chamber. The following primary antibodies were used: rabbit anti-CLDN1 (1:100), anti-

CLDN4 (1:200), anti-LOR (1:200), mouse anti-occludin (1:50), and anti-K4 (1:100). After

rinsing the sections four times with PBS, they were incubated with an anti-mouse or anti-

rabbit immunoglobulin conjugated with Alexa 488 or Alexa 568 (Molecular Probes, Eugene,

OR, USA) at 1:400 dilution in BSA-PBS for 30 min in the dark. The sections were then

washed four times with PBS and mounted in Vectashield mounting medium containing 4′, 6-

diamidino-2-phenylindole (DAPI; Vector Laboratories, Burlingame, CA, USA). The images

were obtained by sequentially scanning the specimen to prevent bleed-through using a

LSM710 confocal laser scanning microscope with the ZEN 2010 software (Carl Zeiss,

Oberkochen, Germany). The system settings were as follows: (1) objective lens: Zeiss Plan-

Apochromat 63×/1.40 Oil DIC M27; fluorescence settings for DAPI: Diode 405-30 laser (405

nm) 4.0%, Channel (Ch) 1, pinhole 67.2 μm (1.0-μm section), filter 415–479 nm; Alexa 488:

Argon laser (488 nm) 5.0%, Ch 1, pinhole 68.5 μm (1.0-μm section), filter 492–545 nm;

Alexa 568: HeNe 543 laser (543 nm) 26.0%, Ch 2, pinhole 64.9 μm (1.0-μm section), filter

555–812 nm; beam splitters: MBS: MBS488/543/633, MBS_InVis: MBS-405; image size:

512 pixel (134.7 μm) × 512 pixel (134.7 μm), pixel size = 0.26 μm; (2) objective lens: Zeiss

EC Plan-Neofluar 20×/0.50 M27; fluorescence settings for DAPI: pinhole 64.9 μm (5.4-μm

section); Alexa 488: pinhole 62.6 μm (5.4-μm section); Alexa 568: pinhole 57.9 μm (5.4-μm

section); image size: 512 pixel (424.3 μm) × 512 pixel (424.3 μm), pixel size = 0.83 μm; other

settings are the same as the 63 × objective lens. Using auto exposure and range indicator,

master gain, digital offset (0.00), and digital gain (1.00–1.24) were determined. Images of the

HE-stained sections were acquired utilizing an Olympus BX51 microscope (Olympus

Corporation, Tokyo, Japan) with an Olympus objective lens (Ach, 60×/0.80) and an interlace

scan CCD camera (Olympus DP12, 3.24 megapixel, 2048 × 1536 pixels resolution).

Gel electrophoresis and immunoblot analysis

The 3D-cultured cells were washed with ice-cold PBS and lysed with 0.2 ml lysis buffer [62.5

mM Tris, pH 6.8, 2% sodium dodecyl sulfate (SDS), 10% glycerol, 5% 2-mercaptoethanol,

and 0.002% bromophenol blue] containing a protease inhibitor cocktail (Sigma-Aldrich) and a

phosphatase inhibitor cocktail (Nacalai Tesque). Cell lysates (10 μl per lane) were

fractionated by SDS-polyacrylamide gel electrophoresis (PAGE) and transferred to

polyvinylidene difluoride (PVDF) membranes. Precision Plus Protein Dual Color Standards

(Bio-Rad, Hercules, CA, USA) were used to determine the size of the detected bands. The

membranes were incubated with Blocking One (Nacalai Tesque) for 1 h and with primary

antibodies overnight at 4°C. Antibodies against CLDN1 (1:1,000), CLDN4 (1:1,000), CLDN7

(1:1,000), and actin (1:2,000) were used as primary antibodies and diluted with Tris-buffered

saline (TBS) [20 mM Tris (pH 7.6) and 137 mM NaCl] containing 5% Blocking One. After

washing with TBS containing 0.1% Tween 20 (T-TBS), the membranes were incubated with

horseradish peroxidase (HRP)-conjugated anti-rabbit or anti-mouse Ig (1:2,000) (GE

Healthcare UK Ltd., Amersham, England) for 1 h. They were then washed with T-TBS, and

the bands were detected using Luminata Forte Western HRP substrate (Millipore, Billerica,

MA, USA). Some membranes were reprobed after stripping the primary and secondary

antibodies with stripping buffer [62.5 mM Tris (pH 6.7), 2% SDS, and 100 mM 2-

mercaptoethanol] at 50°C for 30 min.

Measurement of TER

After 2 weeks of airlift culture, cell culture inserts were transferred to a 24-well plate. CnT-PR

medium containing 1.2 mM calcium was added to the inserts (0.4 ml) and wells (0.6 ml). The

TER was measured using Millicell ERS-2 Voltohmmeter (Millipore). Subsequently, filters

with cultured COCA cells were processed for immunofluorescence microscopy, HE staining,

or immunoblot analysis. TER values were calculated by subtracting the contribution of the

bare filter and medium and multiplying it by the surface area of the filter. All experiments

were performed twice in triplicate.

Statistical analysis

All data are expressed as the mean ± standard error of the mean (SEM). Statistical differences

between the groups were determined by two-sided Welch's *t*-test. $P < 0.05$ was considered

statistically significant.

Results

Both mouse and porcine sera inhibited the keratinization of COCA 3D cultures

We speculated that the concentration of keratinization-suppressing factors in mouse serum

may be lower than that in the sera of cattle and pigs, whose oral cavity epithelia are non-

keratinized. Contrary to our expectation, mouse and porcine sera demonstrated an identical

effect on COCA 3D culture keratinization (Fig. 1). Thus, both mouse and porcine sera

induced parakeratosis at 0.01%, and suppressed keratinization at 0.1% and 1%. Flattened cells

were detected on the surface of 3D cultures treated with 0.1% mouse and porcine sera,

whereas hyperplastic cells were observed after treatment with 1% mouse and porcine sera.

Concerning keratinization, mouse and porcine sera showed the same results as previously

reported for fetal bovine serum (Ozaki et al. 2019).

The keratinization of human, porcine, and mouse keratinocyte 3D cultures was suppressed

by atRA

As shown in Supplementary Fig. 1, pig alveolar mucosa and gingiva include non-keratinized

and keratinized stratified squamous epithelium, respectively. We examined primary

keratinocytes obtained from porcine alveolar mucosa in 3D cultures and found that they

formed keratinized stratified epithelium (Fig. 2a). This suggests that keratinocytes isolated

from non-keratinized epithelium have the capacity to form keratinized epithelium in the 3D

cultures used in this study.

We had previously demonstrated that serum inhibited COCA 3D culture

keratinization, whereas RAR inhibition by BMS 493 restored the keratinization (Ozaki et al.

2019). Therefore, we examined the effect of atRA, a RAR ligand, on the keratinization of 3D

keratinocyte cultures, including primary porcine alveolar mucosal keratinocytes, primary

human epidermal keratinocytes (HEKa), and a mouse epidermal keratinocyte cell line

(COCA). In control 3D cultures, porcine keratinocytes (Fig. 2a), HEKa (Fig. 2d), and COCA

(Fig. 2g) formed keratinized stratified squamous epithelium. After treatment with 0.1 nM

atRA, the cornified layer disappeared, whereas some detaching nucleated cells were present

on the surface of porcine keratinocyte 3D cultures (Fig. 2b) and HEKa (Fig. 2e). However,

COCA still formed the cornified layer although thinner than in a control culture (Fig. 2g),

when treated with 0.1 nM atRA (Fig. 2h). Under treatment with 1 nM atRA, porcine

keratinocytes (Fig. 2c) and HEKa cells (Fig. 2f) formed very thin, unhealthy-looking stratified

epithelium without the cornified layer, whereas COCA cells established non-keratinized

stratified epithelium with some detached nucleated cells on the surface of the 3D cultures

(Fig. 2i). These results suggest that COCA is less susceptible to atRA, which inhibits

keratinization, compared to porcine keratinocytes and HEKa.

The inhibition of RAR signaling restored the keratinization and LOR expression in COCA

3D cultures treated with atRA

COCA 3D cultures treated with DMSO (control), atRA, or atRA plus BMS 493 formed

keratinized, non-keratinized, or keratinized stratified epithelium, respectively (Fig. 3a–c). In

control cultures, LOR was detected in the cells just beneath the cornified layer (Fig. 3d).

When treated with atRA, K4 was observed principally in the suprabasal cells (Fig. 3e). Under

treatment with atRA plus BMS 493, LOR was again detected in the cell layer corresponding

to the granular layer (Fig. 3f). These results indicated that atRA concomitantly inhibited

keratinization and induced K4 protein expression, whereas BMS 493-induced RAR inhibition

simultaneously restored keratinization and induced LOR protein expression.

atRA affected the protein expression and localization of CLDN 1, 4, and 7 and decreased

TER

As atRA affected keratinization and expression of differentiation markers such as K4 and

LOR, we examined tight junction proteins, which represent differentiation markers, because

tight junctions are formed between differentiated keratinocytes. First, we measured the protein

expression of CLDNs 1, 4, and 7 by western blotting (Fig. 4). CLDN4 and CLDN7 were

increased by atRA treatment of COCA 3D cultures, whereas CLDN1 was decreased. BMS

493-induced RAR inhibition restored the expression of CLDN 1, 4, and 7 proteins to the same

levels as in control cultures.

We next examined the immunohistochemical localization of occludin and either CLDN1 (Fig. 5), CLDN4 (Fig. 6), or CLDN7 (Fig. 7). Antibody specificities for occludin, CLDN1, CLDN4, and CLDN7 had been previously reported (Nikaido et al. 2019; Ozaki et al. 2019).

In control cultures (Fig. 5a–c), CLDN1 was detected in the cells just beneath the cornified layer (corresponding to the granular layer cells in the epidermis) as dots or short lines colocalizing with occludin as well as in the cornified layer. When cultures were treated with atRA, CLDN1 disappeared (Fig. 5e). Under treatment with atRA and BMS 493, CLDN1-positive spots reappeared in granular layer cells and in the cornified layer (Fig. 5h) as seen in control.

CLDN4 was colocalized with occludin in granular layer cells as dots or short lines and was also detected in the cornified layer in control cultures (Fig. 6a–c). In addition to spots positive for both CLDN4 and occludin in surface cells, CLDN4 was also observed around the upper half of suprabasal cells when treated with atRA (Fig. 6d–f). CLDN4 around suprabasal cells disappeared after treatment with atRA and BMS 493 (Fig. 6g–i).

CLDN7 was not detected in control cells (Fig. 7a–c). When treated with atRA, CLDN7 was visualized as dots in the cytosol of all cells (basal and suprabasal cells) in non-keratinized stratified epithelium (Fig. 7e), but these CLDN7-positive dots did not colocalize

with occludin (Fig. 7f). CLDN7 disappeared when treated with atRA and BMS 493 (Fig. 7g–

i). The negative immunofluorescence controls in the COCA 3D cultures treated with vehicle

(control), atRA, or atRA plus BMS 493 are shown in Supplementary Fig. 2.

Finally, we assessed the paracellular permeability by TER (Fig. 8). atRA resulted in a

65% decrease in the TER compared to the control; however, RAR inhibition recovered the

TER to the control levels.

Discussion

The esophagus and oral cavity (excluding the gingiva, hard palate, and dorsum of the tongue)

in pig, cattle, and human are covered by non-keratinized stratified squamous epithelium,

whereas those in mouse are covered by keratinized stratified squamous epithelium. Why are

there differences in the keratinization among animal species? One of the possible explanations

is that keratinocytes in non-keratinized epithelium may lose their keratinization ability.

However, this possibility was excluded, because pig keratinocytes obtained from alveolar

mucosa formed keratinized epithelium in 3D cultures. Next, we speculated that mouse serum

might inhibit keratinization less effectively than porcine serum. However, both mouse and

porcine sera exhibited the same inhibitory effect on keratinization at 0.1%. Furthermore, fetal

bovine serum also suppressed keratinization at 0.1% (Ozaki et al. 2019). Altogether, the effect

of serum on keratinization is not substantially different among animal species regardless of

the status of keratinization of the oral and esophageal mucosae.

We further examined the inhibitory effect of atRA on keratinization in 3D keratinocyte cultures of pig, human, and mouse, based on the previous finding that inhibition of keratinization by serum was recovered by the inhibition of RAR (Ozaki et al. 2019). We selected atRA, because retinol in serum is metabolized to atRA, which binds to the RAR in keratinocytes. atRA inhibited keratinization at 0.1 nM in 3D cultures of porcine and human keratinocytes but at 1 nM in those of mouse keratinocytes. These results indicate that mouse keratinocytes need higher atRA concentrations to induce non-keratinized epithelium than porcine and human keratinocytes. This could be one of mechanisms, through which the mouse epithelium in the oral cavity and esophagus is keratinized, although the effect of serum on keratinization is not pronouncedly different among animal species.

We showed that mouse and porcine sera had the same effect on keratinization of COCA 3D cultures, that is, 0.1% serum suppressed keratinization. The atRA concentration in serum in different studies was 1.83–3.99 nM in human (Matsuoka et al. 1991) or 3.59 ± 1.10 nM in mouse, 2.20 ± 1.20 nM in rat, and 4.63 ± 1.00 nM in human (Wolf 2006). Thus, 0.1% mouse serum used in this study would contain 3.59 pM atRA, but keratinization of COCA 3D cultures was not suppressed by this atRA concentration. However, the retinol concentration in serum in different studies was 1.22–2.62 μM in human (Safavi 1992), 0.59 ± 0.03 μM in mouse, 1.82 ± 0.24 μM in rat, and 3.42 ± 0.38 μM in human (Wolf 2006). Regardless of the

dietary daily retinol intake, plasma retinol concentration is maintained at approximately 2 μM

(Blomhoff et al. 1990). Based on these data, 0.1% mouse or porcine serum would contain

approximately 2 nM retinol. We speculated that retinol (~2 nM) in mouse and porcine serum

was incorporated into COCA and metabolized to produce enough atRA (more than 1 nM) in

the cytoplasm to suppress keratinization in this study. If atRA regulates the keratinization of

epidermis and oral mucosa, it is still unclear how the concentration gradient of retinol and

atRA was formed in the tissue fluid surrounding keratinized and non-keratinized epithelium.

As 1 nM atRA suppressed keratinization in our 3D cultures of mouse keratinocytes, the tissue

fluid surrounding mouse epidermis and oral epithelium should be less than 1 nM, although

mouse serum contained 3.59 nM atRA (Wolf 2006). Normal human bronchial epithelial cells,

forming pseudostratified epithelium in vivo, transdifferentiated to non-keratinized stratified

epithelium in 3D cultures by 0.3 nM atRA (Oshima et al. 2011). Therefore, the atRA

concentration in tissue fluid surrounding bronchial epithelium in human should be less than

0.3 nM in order not to induce transdifferentiation in vivo. If this is true, the concentration of

atRA in tissue fluid is less than one sixteenth in serum, 4.63 nM in human (Wolf 2006).

There is a great discrepancy between the effective concentrations of atRA to induce

non-keratinized stratified epithelium in 3D cultures of human keratinocytes: 0.1 nM in this

study versus 100 nM in the previous study (Asselineau et al. 1989). Although our and

previous experiments used human primary keratinocytes, there are several differences

between them: keratinocytes were seeded on filters of culture inserts vs. collagen lattices, the

duration of atRA treatment was 2 weeks vs. 1 week, and culture medium contained no serum

vs. delipidized serum with removed lipid soluble factors including atRA. Serum may likely

cause the discrepancy, because it contains many factors: some induce keratinization, whereas

others suppress it.

atRA increased K4 and decreased LOR protein levels in COCA 3D cultures, whereas

RAR inhibition by BMS 493 reverted them. Consistent with our results, RA induced K4

mRNA and protein expression in vivo and in vitro (Pavez Lorie et al. 2009; Virtanen et al.

2001; Virtanen et al. 2010; Virtanen et al. 2000). K4 upregulation is reportedly a sensitive

marker for retinoid (including atRA) bioactivity in human epidermis (Virtanen et al. 2000).

These findings indicate atRA functioned properly in our 3D culture system.

In our previous study, we speculated that atRA in serum might cause increased

CLDN4 and decreased CLDN1 expression (Ozaki et al. 2019). Actually, we showed that atRA

had the same effect as serum. Furthermore, two reports support the effect of atRA on CLDNs:

atRA increased mRNA and protein levels of CLDN4, but decreased those of CLDN1 in both

human epidermal keratinocytes and mouse epidermis (Li et al. 2019), and in mouse gingival

epithelial cells (Hatakeyama et al. 2010). We further showed that atRA induced CLDN7

protein expression, and that RAR inhibition reverted the change. Consistent with our results,

the claudin7 gene was upregulated in rat embryonic skin after treatment with 1 μM RA for 24

h (Akimoto et al. 2014).

Although atRA induced CLDN7 expression in COCA 3D cultures, it was localized in the cytoplasm in a dotted pattern but not in tight junctions. In contrast, K38 cultured in FAD medium containing 10% fetal bovine serum and probably containing atRA, expressed CLDN7, which was localized in cell–cell borders and tight junctions in 3D cultures (Nikaido et al. 2019). We do not have a clear explanation for the different localization of CLDN7 in COCA and K38, although both cell lines are derived from mouse epidermis. Reportedly, both EpCAM (TROP1) and TACSTD2 (TROP2), which are localized around cell boundaries in stratified epithelium, directly bind to CLDN7 but not to CLDN4 (Kuhn et al. 2007; Ladwein et al. 2005; Nakatsukasa et al. 2010; Nubel et al. 2009). In the cornea of gelatinous drop-like dystrophy, TACSTD2 was not detected around cell boundaries concomitantly with CLDN7 disappearance (Nakatsukasa et al. 2010). Thus, COCA, but not K38, may have lost EpCAM and/or TACSTD2 protein expression.

atRA caused the disappearance of CLDN1 from tight junctions, where occludin was localized, and a 65% decrease in the TER compared with the control. When treated with atRA, CLDN4 was induced to localize around the cell boundaries of suprabasal cell layers in addition to tight junctions, and CLDN7 was expressed in the cytoplasm but not in tight junctions. As occludin was detected only in the surface cells, where tight junctions were formed, CLDN4 localized around the cell boundaries in the deeper cell layers, where occludin

was not detected, may not form tight junctions. Notably, the paracellular permeability barrier in the epidermis was damaged in CLDN1-deficient mice (Furuse et al. 2002). Altogether, atRA reduced the TER by removing CLDN1 from tight junctions. atRA-induced CLDN4 around cell boundaries may not contribute to the increase of TER. Furthermore, RAR inhibition recovered the protein expression and localization of CLDNs 1, 4, and 7 and the TER to the control levels. This suggest that these changes are specifically caused by at RA.

Little is known about the relationship between keratinization and tight junction formation. Both our current and previous (Ozaki et al. 2019) studies showed higher TER in keratinized epithelium than in non-keratinized epithelium due to serum or atRA induction, although there is no direct evidence that keratinization reduced the paracellular permeability. Recently, high enolase-1 expression in the cornified layer has been correlated with insufficient keratinization (parakeratosis) and dysfunction of the tight junction barrier through CLDN4, tricellulin, occludin, and E-cadherin reduction (Tohgasaki et al. 2018). However, there is a discrepancy between these studies: CLDN4 expression was increased by serum or atRA but decreased by enolase-1. In future studies, we will investigate the effect of enolase-1 on our three-dimensional culture system.

Acknowledgements

Conflict of interest

The authors declare that they have no conflict of interest.

References

Akimoto Y, Miyaji M, Morimoto-Kamata R, Kosaka Y, Obinata A (2014) Retinoic acid-

induced epidermal transdifferentiation in skin. J Dev Biol 2:158-173

Asselineau D, Bernard BA, Bailly C, Darmon M (1989) Retinoic acid improves epidermal

morphogenesis. Dev Biol 133:322-335

Babkair H, Yamazaki M, Uddin MS, Maruyama S, Abe T, Essa A, Sumita Y, Ahsan MS,

Swelam W, Cheng J, Saku T (2016) Aberrant expression of the tight junction

molecules claudin-1 and zonula occludens-1 mediates cell growth and invasion in

oral squamous cell carcinoma. Hum Pathol 57:51-60.

https://doi.org/10.1016/j.humpath.2016.07.001

Ban Y, Cooper LJ, Fullwood NJ, Nakamura T, Tsuzuki M, Koizumi N, Dota A, Mochida C,

Kinoshita S (2003a) Comparison of ultrastructure, tight junction-related protein

expression and barrier function of human corneal epithelial cells cultivated on

amniotic membrane with and without air-lifting. Exp Eye Res 76:735-743

Ban Y, Dota A, Cooper LJ, Fullwood NJ, Nakamura T, Tsuzuki M, Mochida C, Kinoshita S

(2003b) Tight junction-related protein expression and distribution in human corneal

epithelium. Exp Eye Res 76:663-669

Blomhoff R, Green MH, Berg T, Norum KR (1990) Transport and storage of vitamin A.

Science 250:399-404. https://doi.org/10.1126/science.2218545

Furuse M, Hata M, Furuse K, Yoshida Y, Haratake A, Sugitani Y, Noda T, Kubo A, Tsukita S

(2002) Claudin-based tight junctions are crucial for the mammalian epidermal

barrier: a lesson from claudin-1-deficient mice. J Cell Biol 156:1099-1111.

https://doi.org/10.1083/jcb.200110122

Furuse M, Sasaki H, Fujimoto K, Tsukita S (1998) A single gene product, claudin-1 or -2,

reconstitutes tight junction strands and recruits occludin in fibroblasts. J Cell Biol

143:391-401

Furuse M, Sasaki H, Tsukita S (1999) Manner of interaction of heterogeneous claudin species

within and between tight junction strands. J Cell Biol 147:891–903

Giguere V, Ong ES, Segui P, Evans RM (1987) Identification of a receptor for the morphogen

retinoic acid. Nature 330:624-629. https://doi.org/10.1038/330624a0

Hatakeyama S, Ishida K, Takeda Y (2010) Changes in cell characteristics due to retinoic acid;

specifically, a decrease in the expression of claudin-1 and increase in claudin-4

within tight junctions in stratified oral keratinocytes. J Periodontal Res 45:207-215.

https://doi.org/10.1111/j.1600-0765.2009.01219.x

Hohl D, Ruf Olano B, de Viragh PA, Huber M, Detrisac CJ, Schnyder UW, Roop DR (1993)

Expression patterns of loricrin in various species and tissues. Differentiation 54:25-

34

Inai T, Kobayashi J, Shibata Y (1999) Claudin-1 contributes to the epithelial barrier function

in MDCK cells. Eur J Cell Biol 78:849-855

Kirschner N, Brandner JM (2012) Barriers and more: functions of tight junction proteins in

the skin. Ann N Y Acad Sci 1257:158-166 doi:10.1111/j.1749-6632.2012.06554.x

Kubo A, Nagao K, Yokouchi M, Sasaki H, Amagai M (2009) External antigen uptake by

Langerhans cells with reorganization of epidermal tight junction barriers. J Exp Med

206:2937-2946. https://doi.org/10.1084/jem.20091527

Kuhn S, Koch M, Nubel T, Ladwein M, Antolovic D, Klingbeil P, Hildebrand D,

Moldenhauer G, Langbein L, Franke WW, Weitz J, Zoller M (2007) A complex of

EpCAM, claudin-7, CD44 variant isoforms, and tetraspanins promotes colorectal

cancer progression. Mol Cancer Res 5:553-567. https://doi.org/10.1158/1541-

7786.MCR-06-0384

Ladwein M, Pape UF, Schmidt DS, Schnolzer M, Fiedler S, Langbein L, Franke WW,

Moldenhauer G, Zoller M (2005) The cell-cell adhesion molecule EpCAM interacts

directly with the tight junction protein claudin-7. Exp Cell Res 309:345-357. https://doi.org/10.1016/j.yexcr.2005.06.013

Li J, Li Q, Geng S (2019) All-trans retinoic acid alters the expression of the tight junction proteins Claudin-1 and -4 and epidermal barrier function-associated genes in the epidermis. Int J Mol Med 43:1789-1805. https://doi.org/10.3892/ijmm.2019.4098

Matsuoka LY, Wortsman J, Tang GW, Russell RM, Parker L, Gelfand R, Mehta RG (1991) Are endogenous retinoids involved in the pathogenesis of acne? Arch Dermatol 127:1072-1073

Moll R, Divo M, Langbein L (2008) The human keratins: biology and pathology. Histochem Cell Biol 129:705-733. https://doi.org/10.1007/s00418-008-0435-6

Morita K, Itoh M, Saitou M, Ando-Akatsuka Y, Furuse M, Yoneda K, Imamura S, Fujimoto K, Tsukita S (1998) Subcellular distribution of tight junction-associated proteins (occludin, ZO-1, ZO-2) in rodent skin. J Invest Dermatol 110:862-866. https://doi.org/10.1046/j.1523-1747.1998.00209.x

Nakatsukasa M, Kawasaki S, Yamasaki K, Fukuoka H, Matsuda A, Tsujikawa M, Tanioka H, Nagata-Takaoka M, Hamuro J, Kinoshita S (2010) Tumor-associated calcium signal transducer 2 is required for the proper subcellular localization of claudin 1 and 7: implications in the pathogenesis of gelatinous drop-like corneal dystrophy. Am J Pathol 177:1344-1355. https://doi.org/10.2353/ajpath.2010.100149

Nikaido M, Otani T, Kitagawa N, Ogata K, Iida H, Anan H, Inai T (2019) Anisomycin, a JNK

and p38 activator, suppresses cell-cell junction formation in 2D cultures of K38

mouse keratinocyte cells and reduces claudin-7 expression, with an increase of

paracellular permeability in 3D cultures. Histochem Cell Biol 151:369-384.

https://doi.org/10.1007/s00418-018-1736-z

Nubel T, Preobraschenski J, Tuncay H, Weiss T, Kuhn S, Ladwein M, Langbein L, Zoller M

(2009) Claudin-7 regulates EpCAM-mediated functions in tumor progression. Mol

Cancer Res 7:285-299. https://doi.org/10.1158/1541-7786.MCR-08-0200

Oshima T, Gedda K, Koseki J, Chen X, Husmark J, Watari J, Miwa H, Pierrou S (2011)

Establishment of esophageal-like non-keratinized stratified epithelium using normal

human bronchial epithelial cells. Am J Physiol Cell Physiol 300:C1422-1429.

https://doi.org/10.1152/ajpcell.00376.2010

Oshima T, Koseki J, Chen X, Matsumoto T, Miwa H (2012) Acid modulates the squamous

epithelial barrier function by modulating the localization of claudins in the superficial

layers. Lab Invest 92:22-31. https://doi.org/10.1038/labinvest.2011.139

Ozaki A, Otani T, Kitagawa N, Ogata K, Iida H, Kojima H, Inai T (2019) Serum affects

keratinization and tight junctions in three-dimensional cultures of the mouse

keratinocyte cell line COCA through retinoic acid receptor-mediated signaling.

Histochem Cell Biol 151:315-326. https://doi.org/10.1007/s00418-018-1741-2

Pavez Lorie E, Chamcheu JC, Vahlquist A, Torma H (2009) Both all-trans retinoic acid and

cytochrome P450 (CYP26) inhibitors affect the expression of vitamin A metabolizing

enzymes and retinoid biomarkers in organotypic epidermis. Arch Dermatol Res

301:475-485. https://doi.org/10.1007/s00403-009-0937-7

Safavi K (1992) Serum vitamin A levels in psoriasis: results from the First National Health

and Nutrition Examination Survey. Arch Dermatol 128:1130-1131

Segrelles C, Holguin A, Hernandez P, Ariza JM, Paramio JM, Lorz C (2011) Establishment of

a murine epidermal cell line suitable for in vitro and in vivo skin modelling. BMC

Dermatol 11:9. https://doi.org/10.1186/1471-5945-11-9

Seo A, Kitagawa N, Matsuura T, Sato H, Inai T (2016) Formation of keratinocyte multilayers

on filters under airlifted or submerged culture conditions in medium containing

calcium, ascorbic acid, and keratinocyte growth factor. Histochem Cell Biol 146:585-

597. https://doi.org/10.1007/s00418-016-1472-1

Takaoka M, Nakamura T, Ban Y, Kinoshita S (2007) Phenotypic investigation of cell junction-

related proteins in gelatinous drop-like corneal dystrophy. Invest Ophthalmol Vis Sci

48:1095-1101. https://doi.org/10.1167/iovs.06-0740

Tohgasaki T, Ozawa N, Yoshino T, Ishiwatari S, Matsukuma S, Yanagi S, Fukuda H (2018)

Enolase-1 expression in the stratum corneum is elevated with parakeratosis of atopic

dermatitis and disrupts the cellular tight junction barrier in keratinocytes. Int J

Cosmet Sci 40:178-186. https://doi.org/10.1111/ics.12449

Tsuruta D, Green KJ, Getsios S, Jones JC (2002) The barrier function of skin: how to keep a

tight lid on water loss. Trends Cell Biol 12:355-357

Virtanen M, Gedde-Dahl T, Jr., Mork NJ, Leigh I, Bowden PE, Vahlquist A (2001)

Phenotypic/genotypic correlations in patients with epidermolytic hyperkeratosis and

the effects of retinoid therapy on keratin expression. Acta Derm Venereol 81:163-

170. https://doi.org/10.1080/000155501750376221

Virtanen M, Sirsjo A, Vahlquist A, Torma H (2010) Keratins 2 and 4/13 in reconstituted

human skin are reciprocally regulated by retinoids binding to nuclear receptor

RARalpha. Exp Dermatol 19:674-681. https://doi.org/10.1111/j.1600-

0625.2010.01079.x

Virtanen M, Torma H, Vahlquist A (2000) Keratin 4 upregulation by retinoic acid in vivo: a

sensitive marker for retinoid bioactivity in human epidermis. J Invest Dermatol

114:487-493. https://doi.org/10.1046/j.1523-1747.2000.00901.x

Wolf G (2006) Is 9-cis-retinoic acid the endogenous ligand for the retinoic acid-X receptor?

Nutr Rev 64:532-538. https://doi.org/10.1111/j.1753-4887.2006.tb00186.x

Yoshida Y, Ban Y, Kinoshita S (2009) Tight junction transmembrane protein claudin subtype

expression and distribution in human corneal and conjunctival epithelium. Invest

Ophthalmol Vis Sci 50:2103-2108. https://doi.org/10.1167/iovs.08-3046

Yu AS, Cheng MH, Angelow S, Günzel D, Kanzawa SA, Schneeberger EE, Fromm M,

Coalson RD (2009) Molecular basis for cation selectivity in claudin-2-based

paracellular pores: identification of an electrostatic interaction site. J Gen Physiol

133:111-127. https://doi.org/10.1085/jgp.200810154.

Akimoto Y, Miyaji M, Morimoto-Kamata R, Kosaka Y, Obinata A (2014) Retinoic acid-

induced epidermal transdifferentiation in skin. J Dev Biol 2:158-173

Asselineau D, Bernard BA, Bailly C, Darmon M (1989) Retinoic acid improves epidermal

morphogenesis. Dev Biol 133:322-335

Babkair H, Yamazaki M, Uddin MS, Maruyama S, Abe T, Essa A, Sumita Y, Ahsan MS,

Swelam W, Cheng J, Saku T (2016) Aberrant expression of the tight junction

molecules claudin-1 and zonula occludens-1 mediates cell growth and invasion in

oral squamous cell carcinoma. Hum Pathol 57:51-60.

https://doi.org/10.1016/j.humpath.2016.07.001

Ban Y, Cooper LJ, Fullwood NJ, Nakamura T, Tsuzuki M, Koizumi N, Dota A, Mochida C,

Kinoshita S (2003a) Comparison of ultrastructure, tight junction-related protein

expression and barrier function of human corneal epithelial cells cultivated on

amniotic membrane with and without air-lifting. Exp Eye Res 76:735-743

Ban Y, Dota A, Cooper LJ, Fullwood NJ, Nakamura T, Tsuzuki M, Mochida C, Kinoshita S

(2003b) Tight junction-related protein expression and distribution in human corneal

epithelium. Exp Eye Res 76:663-669

Blomhoff R, Green MH, Berg T, Norum KR (1990) Transport and storage of vitamin A.

Science 250:399-404. https://doi.org/10.1126/science.2218545

Furuse M, Hata M, Furuse K, Yoshida Y, Haratake A, Sugitani Y, Noda T, Kubo A, Tsukita S

(2002) Claudin-based tight junctions are crucial for the mammalian epidermal

barrier: a lesson from claudin-1-deficient mice. J Cell Biol 156:1099-1111.

https://doi.org/10.1083/jcb.200110122

Furuse M, Sasaki H, Fujimoto K, Tsukita S (1998) A single gene product, claudin-1 or -2,

reconstitutes tight junction strands and recruits occludin in fibroblasts. J Cell Biol

143:391-401

Furuse M, Sasaki H, Tsukita S (1999) Manner of interaction of heterogeneous claudin species

within and between tight junction strands. J Cell Biol. 147:891–903.

Giguere V, Ong ES, Segui P, Evans RM (1987) Identification of a receptor for the morphogen

retinoic acid. Nature 330:624-629. https://doi.org/10.1038/330624a0

Hatakeyama S, Ishida K, Takeda Y (2010) Changes in cell characteristics due to retinoic acid;

specifically, a decrease in the expression of claudin-1 and increase in claudin-4

within tight junctions in stratified oral keratinocytes. J Periodontal Res 45:207-215.

https://doi.org/10.1111/j.1600-0765.2009.01219.x

Hohl D, Ruf Olano B, de Viragh PA, Huber M, Detrisac CJ, Schnyder UW, Roop DR (1993) Expression patterns of loricrin in various species and tissues. Differentiation 54:25-34

Inai T, Kobayashi J, Shibata Y (1999) Claudin-1 contributes to the epithelial barrier function in MDCK cells. Eur J Cell Biol 78:849-855.

Kirschner N, Brandner JM (2012) Barriers and more: functions of tight junction proteins in the skin. Ann N Y Acad Sci 1257:158-166 doi:10.1111/j.1749-6632.2012.06554.x

Kubo A, Nagao K, Yokouchi M, Sasaki H, Amagai M (2009) External antigen uptake by Langerhans cells with reorganization of epidermal tight junction barriers. J Exp Med 206:2937-2946. https://doi.org/10.1084/jem.20091527

Kuhn S, Koch M, Nubel T, Ladwein M, Antolovic D, Klingbeil P, Hildebrand D, Moldenhauer G, Langbein L, Franke WW, Weitz J, Zoller M (2007) A complex of EpCAM, claudin-7, CD44 variant isoforms, and tetraspanins promotes colorectal cancer progression. Mol Cancer Res 5:553-567. https://doi.org/10.1158/1541-7786.MCR-06-0384

Ladwein M, Pape UF, Schmidt DS, Schnolzer M, Fiedler S, Langbein L, Franke WW, Moldenhauer G, Zoller M (2005) The cell-cell adhesion molecule EpCAM interacts directly with the tight junction protein claudin-7. Exp Cell Res 309:345-357.

https://doi.org/10.1016/j.yexcr.2005.06.013

Li J, Li Q, Geng S (2019) All-trans retinoic acid alters the expression of the tight junction

proteins Claudin-1 and -4 and epidermal barrier function-associated genes in the

epidermis. Int J Mol Med 43:1789-1805. https://doi.org/10.3892/ijmm.2019.4098

Matsuoka LY, Wortsman J, Tang GW, Russell RM, Parker L, Gelfand R, Mehta RG (1991)

Are endogenous retinoids involved in the pathogenesis of acne? Arch Dermatol

127:1072-1073

Moll R, Divo M, Langbein L (2008) The human keratins: biology and pathology. Histochem

Cell Biol 129:705-733. https://doi.org/10.1007/s00418-008-0435-6

Morita K, Itoh M, Saitou M, Ando-Akatsuka Y, Furuse M, Yoneda K, Imamura S, Fujimoto

K, Tsukita S (1998) Subcellular distribution of tight junction-associated proteins

(occludin, ZO-1, ZO-2) in rodent skin. J Invest Dermatol 110:862-866.

https://doi.org/10.1046/j.1523-1747.1998.00209.x

Nakatsukasa M, Kawasaki S, Yamasaki K, Fukuoka H, Matsuda A, Tsujikawa M, Tanioka H,

Nagata-Takaoka M, Hamuro J, Kinoshita S (2010) Tumor-associated calcium signal

transducer 2 is required for the proper subcellular localization of claudin 1 and 7:

implications in the pathogenesis of gelatinous drop-like corneal dystrophy. Am J

Pathol 177:1344-1355. https://doi.org/10.2353/ajpath.2010.100149

Nikaido M, Otani T, Kitagawa N, Ogata K, Iida H, Anan H, Inai T (2019) Anisomycin, a JNK

34

and p38 activator, suppresses cell-cell junction formation in 2D cultures of K38

mouse keratinocyte cells and reduces claudin-7 expression, with an increase of

paracellular permeability in 3D cultures. Histochem Cell Biol 151:369-384.

https://doi.org/10.1007/s00418-018-1736-z

Nubel T, Preobraschenski J, Tuncay H, Weiss T, Kuhn S, Ladwein M, Langbein L, Zoller M

(2009) Claudin-7 regulates EpCAM-mediated functions in tumor progression. Mol

Cancer Res 7:285-299. https://doi.org/10.1158/1541-7786.MCR-08-0200

Oshima T, Gedda K, Koseki J, Chen X, Husmark J, Watari J, Miwa H, Pierrou S (2011)

Establishment of esophageal-like non-keratinized stratified epithelium using normal

human bronchial epithelial cells. Am J Physiol Cell Physiol 300:C1422-1429.

https://doi.org/10.1152/ajpcell.00376.2010

Oshima T, Koseki J, Chen X, Matsumoto T, Miwa H (2012) Acid modulates the squamous

epithelial barrier function by modulating the localization of claudins in the superficial

layers. Lab Invest 92:22-31. https://doi.org/10.1038/labinvest.2011.139

Ozaki A, Otani T, Kitagawa N, Ogata K, Iida H, Kojima H, Inai T (2019) Serum affects

keratinization and tight junctions in three-dimensional cultures of the mouse

keratinocyte cell line COCA through retinoic acid receptor-mediated signaling.

Histochem Cell Biol 151:315-326. https://doi.org/10.1007/s00418-018-1741-2

Pavez Lorie E, Chamcheu JC, Vahlquist A, Torma H (2009) Both all-trans retinoic acid and

cytochrome P450 (CYP26) inhibitors affect the expression of vitamin A metabolizing

enzymes and retinoid biomarkers in organotypic epidermis. Arch Dermatol Res

301:475-485. https://doi.org/10.1007/s00403-009-0937-7

Safavi K (1992) Serum vitamin A levels in psoriasis: results from the First National Health

and Nutrition Examination Survey. Arch Dermatol 128:1130-1131

Segrelles C, Holguin A, Hernandez P, Ariza JM, Paramio JM, Lorz C (2011) Establishment of

a murine epidermal cell line suitable for in vitro and in vivo skin modelling. BMC

Dermatol 11:9. https://doi.org/10.1186/1471-5945-11-9

Seo A, Kitagawa N, Matsuura T, Sato H, Inai T (2016) Formation of keratinocyte multilayers

on filters under airlifted or submerged culture conditions in medium containing

calcium, ascorbic acid, and keratinocyte growth factor. Histochem Cell Biol 146:585-

597. https://doi.org/10.1007/s00418-016-1472-1

Takaoka M, Nakamura T, Ban Y, Kinoshita S (2007) Phenotypic investigation of cell junction-

related proteins in gelatinous drop-like corneal dystrophy. Invest Ophthalmol Vis Sci

48:1095-1101. https://doi.org/10.1167/iovs.06-0740

Tohgasaki T, Ozawa N, Yoshino T, Ishiwatari S, Matsukuma S, Yanagi S, Fukuda H (2018)

Enolase-1 expression in the stratum corneum is elevated with parakeratosis of atopic

dermatitis and disrupts the cellular tight junction barrier in keratinocytes. Int J

Cosmet Sci 40:178-186. https://doi.org/10.1111/ics.12449

Tsuruta D, Green KJ, Getsios S, Jones JC (2002) The barrier function of skin: how to keep a

    tight lid on water loss. Trends Cell Biol 12:355-357

Virtanen M, Gedde-Dahl T, Jr., Mork NJ, Leigh I, Bowden PE, Vahlquist A (2001)

    Phenotypic/genotypic correlations in patients with epidermolytic hyperkeratosis and

    the effects of retinoid therapy on keratin expression. Acta Derm Venereol 81:163-

    170. https://doi.org/10.1080/000155501750376221

Virtanen M, Sirsjo A, Vahlquist A, Torma H (2010) Keratins 2 and 4/13 in reconstituted

    human skin are reciprocally regulated by retinoids binding to nuclear receptor

    RARalpha. Exp Dermatol 19:674-681. https://doi.org/10.1111/j.1600-

    0625.2010.01079.x

Virtanen M, Torma H, Vahlquist A (2000) Keratin 4 upregulation by retinoic acid in vivo: a

    sensitive marker for retinoid bioactivity in human epidermis. J Invest Dermatol

    114:487-493. https://doi.org/10.1046/j.1523-1747.2000.00901.x

Wolf G (2006) Is 9-cis-retinoic acid the endogenous ligand for the retinoic acid-X receptor?

    Nutr Rev 64:532-538. https://doi.org/10.1111/j.1753-4887.2006.tb00186.x

Yoshida Y, Ban Y, Kinoshita S (2009) Tight junction transmembrane protein claudin subtype

    expression and distribution in human corneal and conjunctival epithelium. Invest

    Ophthalmol Vis Sci 50:2103-2108. https://doi.org/10.1167/iovs.08-3046

Yu AS, Cheng MH, Angelow S, Günzel D, Kanzawa SA, Schneeberger EE, Fromm M,

Coalson RD (2009) Molecular basis for cation selectivity in claudin-2-based paracellular

pores: identification of an electrostatic interaction site. J Gen Physiol 133:111-127.

https://doi.org/10.1085/jgp.200810154

Figure legends

Fig. 1 Mouse and porcine sera exerted the same suppressive effect on the keratinization in

COCA 3D cultures. COCA cells seeded on the filters of cell culture inserts were airlifted for 2

weeks in the presence of 0.01% (a, d), 0.1% (b, e), or 1% (c, f) mouse (a–c) or porcine (d–f)

serum. Morphology of 3D cultures was examined after HE staining. Flattened nuclei were

observed in the cornified layer (parakeratosis), when cells were treated with 0.01% serum (a,

d). Non-keratinized stratified squamous epithelium, where several layers of flattened cells

were on the top of 3D cultures, was formed under treatment with 0.1% serum (b, e). When

cultures were treated with 1% serum, hyperplastic cells were detected on the surface of 3D

cultures, and cell-cell junctions were enlarged (c, f). Scale bar: 20 μm for all images.

Fig. 2 Effect of atRA on 3D cultures of porcine mucosal keratinocytes, HEKa, or COCA.

Cells seeded on the filters of cell culture inserts were airlifted for 2 weeks in the presence of

0.1% DMSO as a control (a, d, g), 0.1 nM atRA (b, e, h), or 1 nM atRA (c, f, i). Morphology

of 3D cultures was examined after HE staining. The cornified layer indicated by a white

vertical line was observed (a, d, g, h). Flattened nuclei designated by arrows were detected in the surface layers (b, e). Hyperplastic and detaching cells (arrowheads in b, e, i) were observed on the surface of 3D cultures. When cultures were treated with 0.1 nM atRA, porcine keratinocytes (b) and HEKa (e) formed non-keratinized stratified squamous epithelium, whereas COCA still formed keratinized stratified squamous epithelium (h). Under treatment with 1 nM atRA, porcine keratinocytes (c) and HEKa (f) formed very thin, unhealthy-appearing non-keratinized epithelium, whereas COCA established non-keratinized stratified squamous epithelium with many detached hyperplastic cells (i). Scale bar: 20 μm for all images.

Fig. 3 atRA affected the keratinization and expression of keratinocyte differentiation markers in COCA 3D cultures. COCA cultures were airlifted for 2 weeks in the presence of 0.1% DMSO (a, d), 1 nM atRA (b, e), or 1nM atRA plus 0.2 μM BMS 493 (c, f). They were stained with HE (a–c) or immunolabeled with K4 and LOR (d–f). Nuclei were stained with DAPI (blue). COCA 3D cultures treated with DMSO, atRA, or atRA plus BMS 493 formed keratinized (a), non-keratinized (b), or keratinized (c) stratified epithelium, respectively. In control cultures, LOR (red) was localized in cells just beneath the cornified layer, whereas K4 (green) was not detected (d). atRA induced K4 but suppressed LOR protein expression (e). BMS 493-induced RAR inhibition suppressed K4 but induced LOR expression (f). Scale bars

in c and f: 20 μm for a–c and d–f, respectively.

Fig. 4 atRA affected the protein expression of CLDN 1, 4, and 7 in COCA 3D cultures.
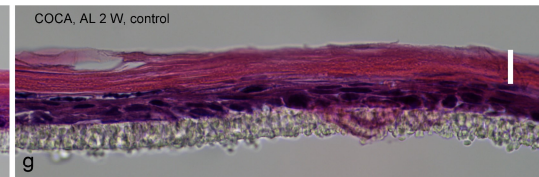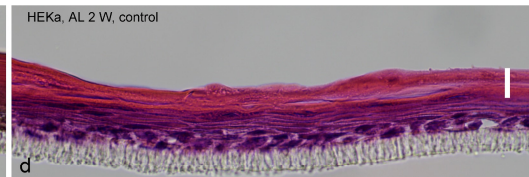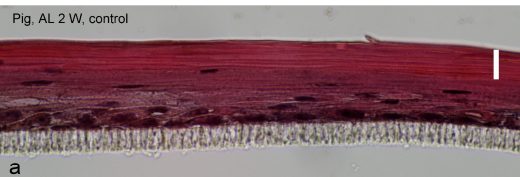
COCA cultures were airlifted for 2 weeks in the presence of 0.1% DMSO (control), 1 nM

atRA, or 1nM atRA plus 0.2 μM BMS 493 and analyzed by immunoblotting. atRA reduced

CLDN1 but increased CLDN4 expression. CLDN7 was not detected in control cells but was

induced by atRA treatment. BMS 493 recovered the CLDN expression pattern to the control

levels.

Fig. 5 atRA suppressed the protein expression of CLDN1 in COCA 3D cultures. COCA

cultures were airlifted for 2 weeks in the presence of 0.1% DMSO (a–c), 1 nM atRA (d–f), or

1 nM atRA plus 0.2 μM BMS 493 (g–i) and double-immunostained with occludin (green) and

CLDN1 (red). Merged images are shown in c, f, and i. Nuclei were stained with DAPI (blue).

In control cultures, occludin-positive spots were observed in cells just beneath the cornified

layer and were colocalized with CLDN1 (arrows in a–c). In addition, CLDN1 was detected in

the cornified layer (b). When cells were treated with atRA, CLDN1 signals almost

disappeared (e), whereas occludin localization was not altered (d). BMS 493 recovered the

CLDN1 localization and its colocalization with occludin (arrows in g–i). Scale bar: 20 μm for

all images.

Fig. 6 atRA altered the localization of CLDN4 in COCA 3D cultures. COCA cultures were airlifted for 2 weeks in the presence of 0.1% DMSO (a–c), 1 nM atRA (d–f), or 1 nM atRA plus 0.2 μM BMS 493 (g–i) and double-immunostained with occludin (green) and CLDN4 (red). Merged images are shown in c, f, and i. Nuclei were stained with DAPI (blue). In control cultures, occludin-positive spots were observed in cells just beneath the cornified layer and were colocalized with CLDN4 (arrows in a–c). In addition, CLDN4 was detected in the cornified layer (b). When the cultures were treated with atRA, CLDN4 was detected around the cell boundaries in the upper half of the stratified cell layers (e), in addition to the surface cells, where CLDN4 was colocalized with occludin (arrows in d–f). BMS 493 recovered the CLDN4 localization and its colocalization with occludin in the granular layer cells (arrows in g–i). Scale bar: 20 μm for all images.

Fig. 7 atRA induced the protein expression of CLDN7 in COCA 3D cultures. COCA cultures were airlifted for 2 weeks in the presence of 0.1% DMSO (a–c), 1 nM atRA (d–f), or 1 nM atRA plus 0.2 μM BMS 493 (g–i) and double-immunostained with occludin (green) and CLDN7 (red). Merged images are shown in c, f, and i. Nuclei were stained with DAPI (blue). In control cultures, occludin-positive spots were observed in cells just beneath the cornified layer (a), whereas CLDN7 was not detected (b). When cells were treated with atRA, signals

for CLDN7 were observed in the cytoplasm in a dot-like pattern (e) but were not colocalized

with occludin-positive spots (f). BMS 493 suppressed CLDN7 (h) but not occludin expression

(g). Scale bar: 20 μm for all images.

Fig. 8 atRA-induced TER reduction in 3D COCA cultures. COCA cultures were airlifted for 2

weeks in the presence of 0.1% DMSO (control), 1 nM atRA, or 1 nM atRA plus 0.2 μM BMS

493, and the TER was measured. atRA reduced the TER by 65% compared with the control,

whereas RAR inhibition recovered the TER to the control level. Values are expressed as the

mean $\pm$ SEM. *$P < 0.05$ vs control.

Supplementary Fig. 1 Morphology of the mucogingival junction of pig mandible. The

mucogingival junction of pig mandible was fixed with 1% paraformaldehyde and embedded

in an OCT compound. Cryosections were stained with HE. An arrow (a) indicates the

boundary between non-keratinized lingual alveolar mucosa (the left-hand side) and

keratinized lingual gingiva (the right-hand side). A high magnification photomicrograph of

non-keratinized alveolar mucosa (b) or keratinized gingiva (c) is shown. Scale bars in a–c:

100 μm.

Supplementary Fig. 2 Negative controls for immunofluorescence in COCA 3D cultures.

COCA cells seeded on insert filters were airlifted for 2 weeks in the presence of 0.1% DMSO

as a control (a–c), 1 nM atRA (d–f), or 1 nM atRA plus 0.2 μM BMS 493 (g–i). Cryosections

were incubated with BSA-PBS in place of primary antibodies and then incubated with

secondary antibodies (a mixture of anti-mouse Ig conjugated with Alexa 488 and anti-rabbit

Ig conjugated with Alexa 568). Nuclei were stained with DAPI (blue). Images derived from

Alexa 488 (green) are shown in a, d, and g. Images derived from Alexa 568 (red) are

presented in b, e, and h. Merged images are shown in c, f, and i. No specific signals were

observed in these controls. Scale bar: 20 μm.

COCA, AL 2 W — a: 0.01% mouse serum; b: 0.1% mouse serum; c: 1% mouse serum; d: 0.01% pig serum; e: 0.1% pig serum; f: 1% pig serum. Scale bar: 20 um

Pig, AL 2 W, control

0.1 nM atRA

1 nM atRA

HEKa, AL 2 W, control
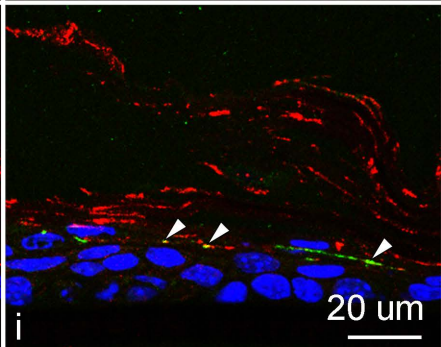
COCA, AL 2 W, control

a

b
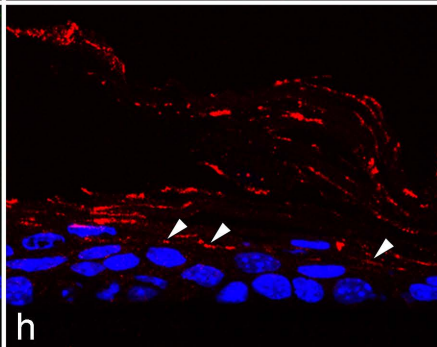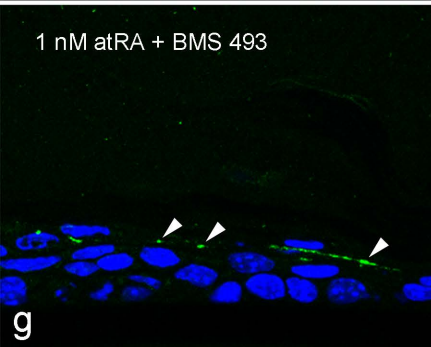
c

d

e

f

g

h

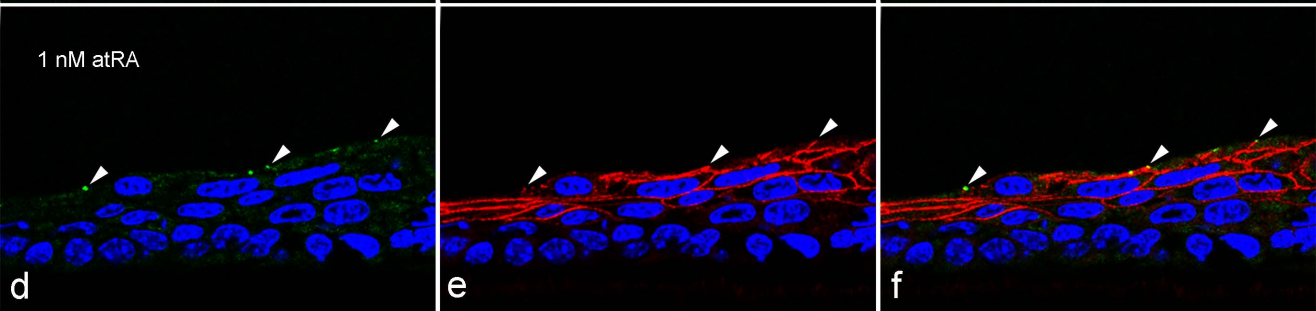i

20 um
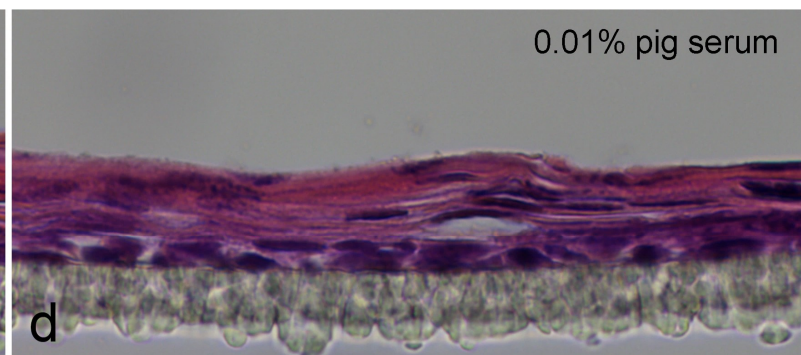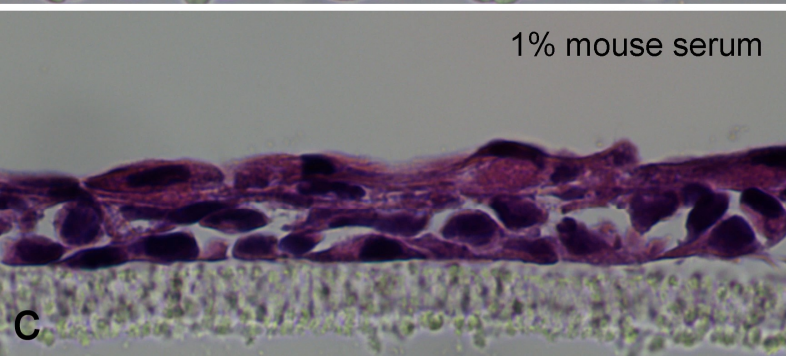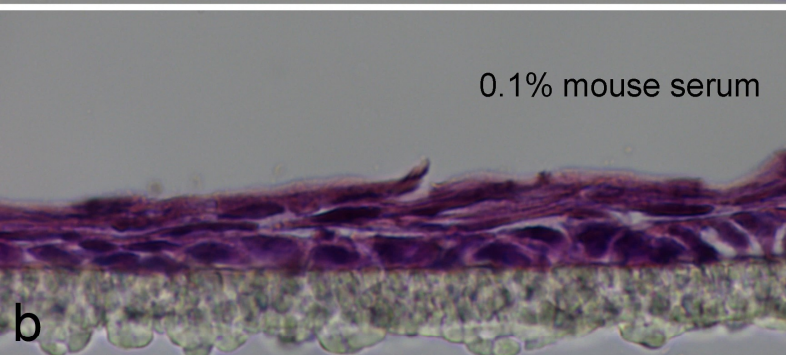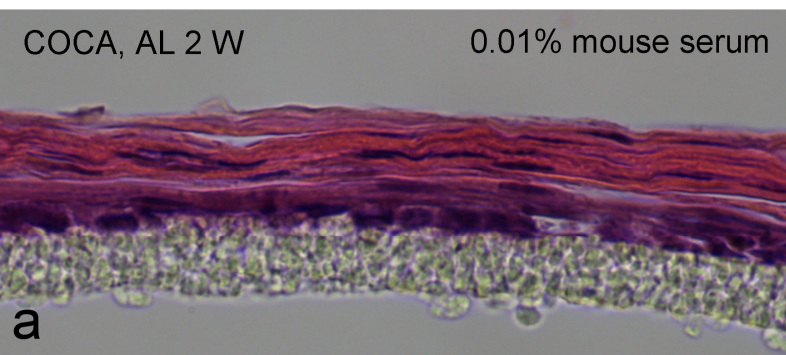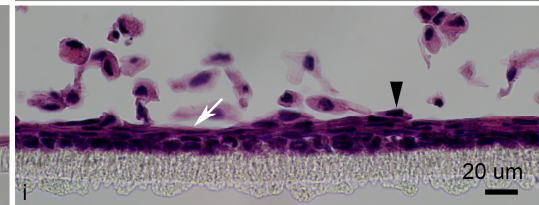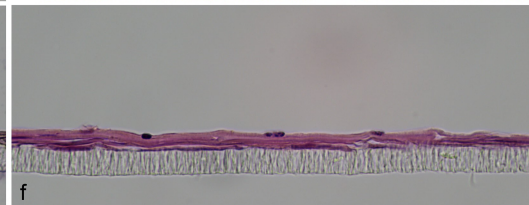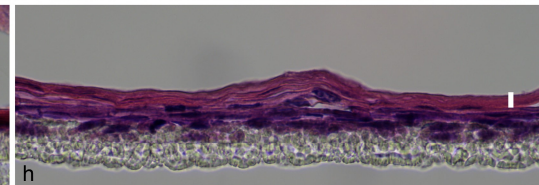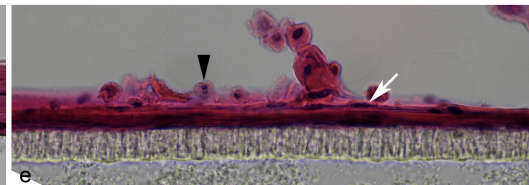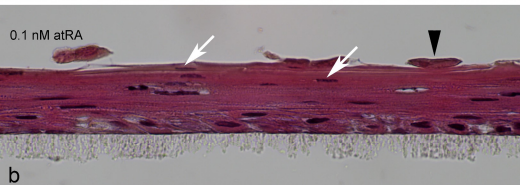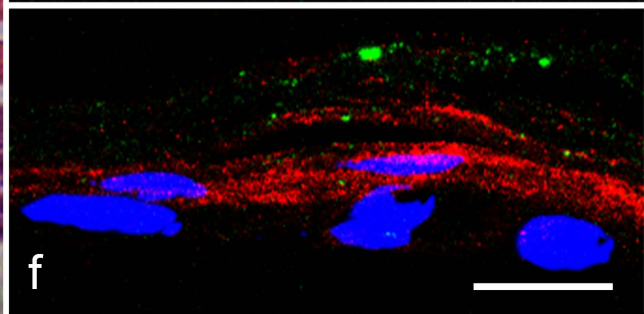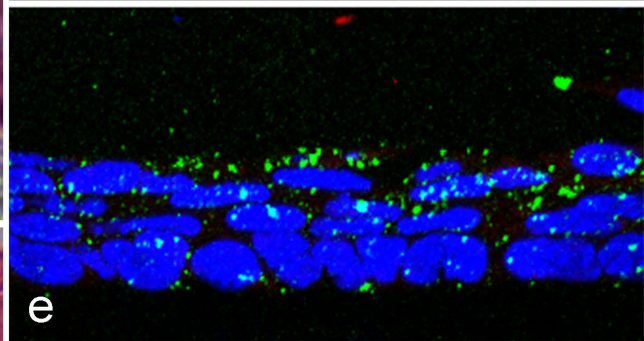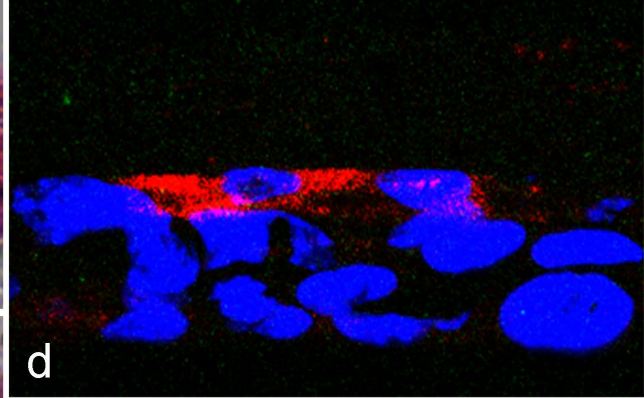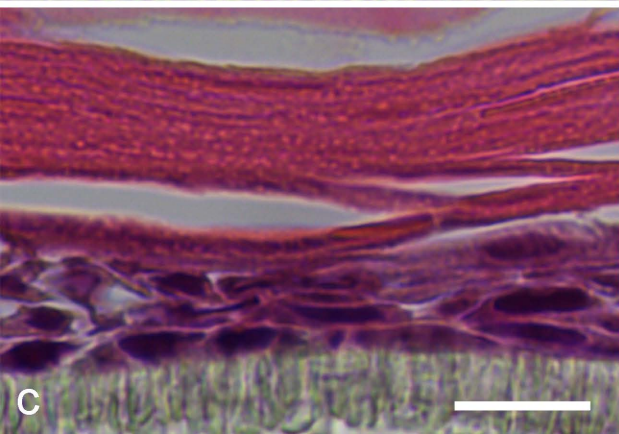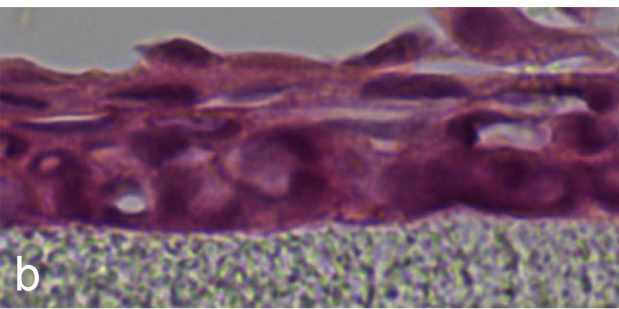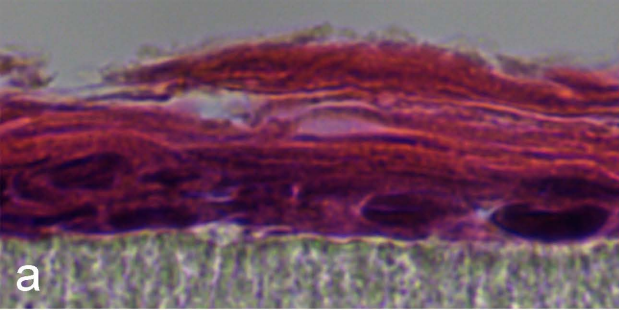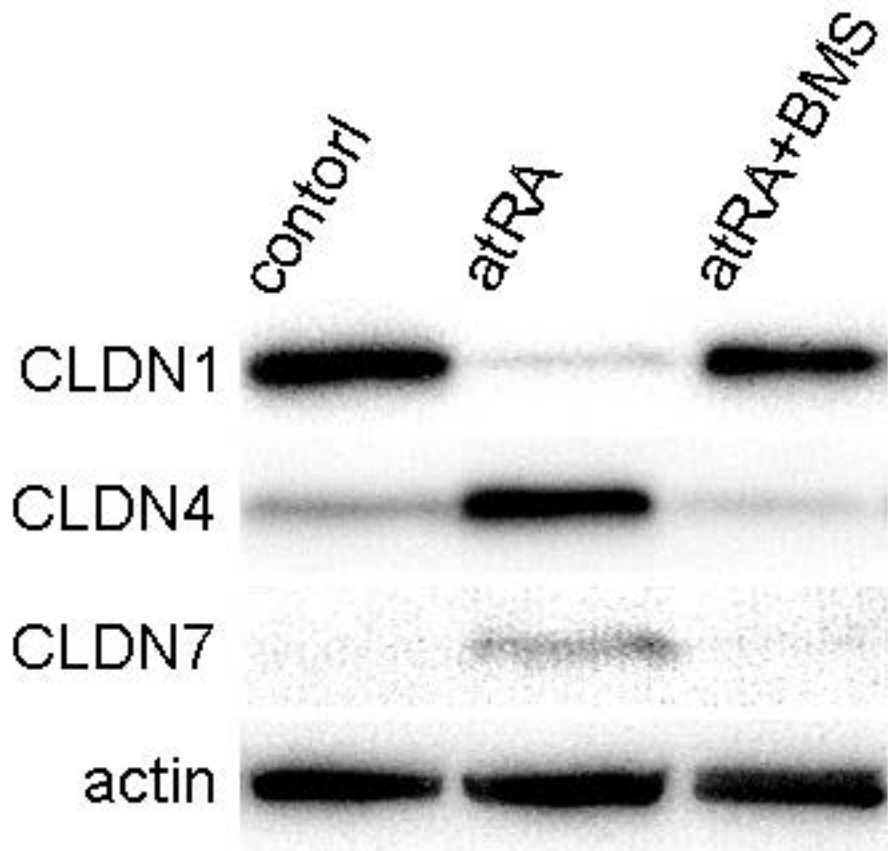
COCA 2 W, OC+CLDN1
control
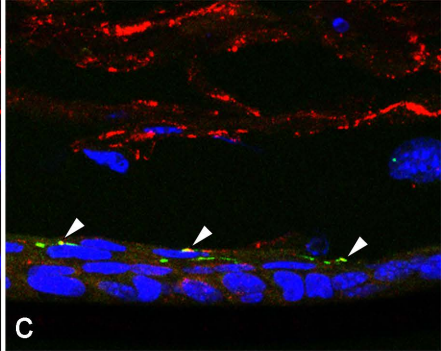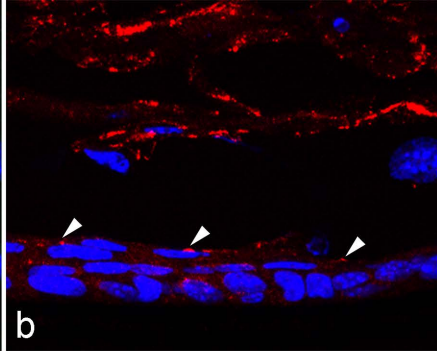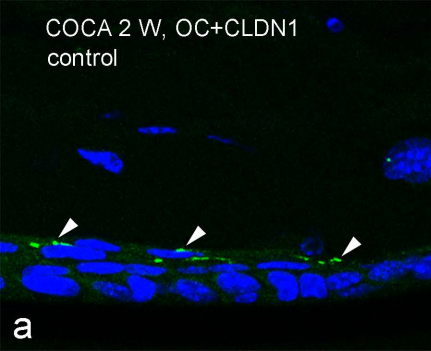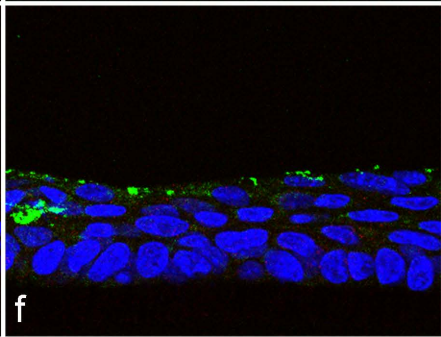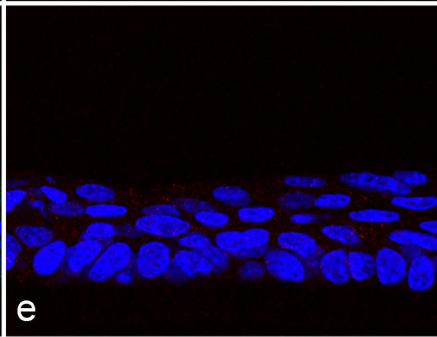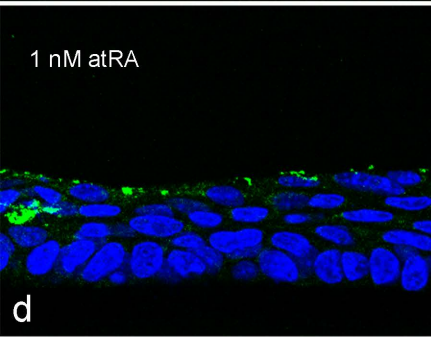
1 nM atRA
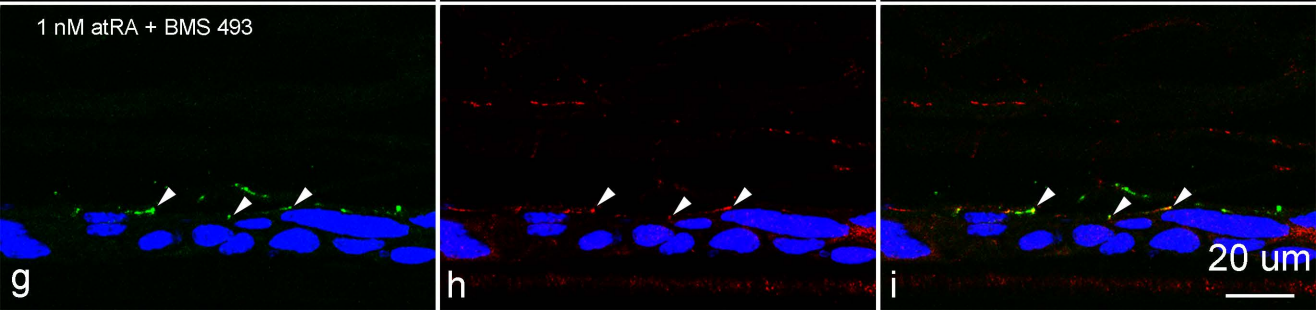
1 nM atRA + BMS 493

20 um

COCA 2 W, OC+CLDN4

OC+CLDN7

COCA 2 W, Control

atRA

atRA+BMS

20 um

Negative Control without primary antibody

Control

1 nM atRA

1 nM atRA + 0.2 uM BMS 493